Research Article

Journal of Molecular Microbiology and Biotechnology

J Mol Microbiol Biotechnol 2010;19:213–223
DOI: 10.1159/000320697

Published online: December 14, 2010

The 6-Phosphogluconate Dehydrogenase of *Leishmania (Leishmania) mexicana*: Gene Characterization and Protein Structure Prediction

Deyanira González[a] José Luis Pérez[a] María Luisa Serrano[b]
Mariana Igoillo-Esteve[c] Juan José Cazzulo[c] Michael P. Barrett[d] José Bubis[e]
Alexis Mendoza-León[a]

[a]Laboratorio de Bioquímica y Biología Molecular de Parásitos, Instituto de Biología Experimental (IBE), Facultad de Ciencias, y [b]Unidad de Química Medicinal, Facultad de Farmacia, Universidad Central de Venezuela, Caracas, Venezuela; [c]Instituto de Investigaciones Biotecnológicas/INTECH, Universidad Nacional General San Martín/CONICET, Buenos Aires, Argentina; [d]Division of Infection and Immunity and Wellcome Centre for Molecular Parasitology, Glasgow Biomedical Research Centre, University of Glasgow, Glasgow, UK; [e]Departamento de Biología Celular, Universidad Simón Bolívar, Caracas, Venezuela

Key Words
Leishmania · Pentose phosphate pathway · 6-Phosphogluconate dehydrogenase · Three-dimensional structure

Abstract
6-Phosphogluconate dehydrogenase (6PGDH) is a key enzyme of the oxidative branch involved in the generation of NADPH and ribulose 5-phosphate. In the present work, we describe the cloning, sequencing and characterization of a 6PGDH gene from *Leishmania (Leishmania) mexicana*. The gene encodes a polypeptide chain of 479 amino acid residues with a predicted molecular mass of 52 kDa and a pI of 5.77. The recombinant protein possesses a dimeric quaternary structure and displays kinetic parameter values intermediate between those reported for *Trypanosoma brucei* and *T. cruzi* with apparent K_m values of 6.93 and 5.2 μM for 6PG and $NADP^+$, respectively. The three-dimensional structure of the enzymes of *Leishmania* and *T. cruzi* were modelled from their amino acid sequence using the crystal structure of the enzyme of *T. brucei* as template. The amino acid residues located in the 6PGDH C-terminal region, which are known to participate in the salt bridges maintaining the protein dimeric structure, differed significantly among the enzymes of *Leishmania*, *T. cruzi*, and *T. brucei*. Our results strongly suggest that 6PGDH can be selected as a potential target for the development of new therapeutic drugs in order to improve existing chemotherapeutic treatments against these parasites.

Introduction

Leishmaniasis is a complex disease whose causative agents are protozoan parasites of the genus *Leishmania* that produce a variety of clinical and pathological manifestations (cutaneous, mucosal and visceral). The disease is distributed worldwide and remains a major public health problem mainly in the tropical and subtropical regions, with an estimated prevalence of 12 million cases.

KARGER

Fax +41 61 306 12 34
E-Mail karger@karger.ch
www.karger.com

1464–1801/10/0194–0213$26.00/0

Accessible online at:
www.karger.com/mmb

A. Mendoza-León, PhD
Instituto de Biología Experimental (IBE), Universidad Central de Venezuela
Caracas 1041 (Venezuela)
Tel./Fax +58 212 753 5897, E-Mail amendoza50@gmail.com

In the absence of effective vaccines, chemotherapy has been the mainstay for treatment of the disease; the chemotherapy currently available relies on the administration of antimonial compounds, such as meglumine antimoniate (Glucantime) or sodium stibogluconate (Pentostam) [Croft and Coombs, 2003; Ouellette et al., 2004]. However, the toxicity of these drugs, a lack of knowledge of their mechanisms of action, the intrinsic differences in drug-sensitivity between *Leishmania* species and the emergence and spread of drug resistance underlie an urgent need for affordable alternative drugs or novel vaccines for prevention and control of the disease [Coler et al., 2005; Croft and Coombs, 2003; Davis et al., 2004]. The most significant therapeutic advance has been the introduction of the first effective oral treatment with miltefosine, an alkyl-lysophospholipid, which has produced high cure rates in patients with visceral leishmaniasis [Croft et al., 2005]. Recently, it has been demonstrated that the combination of miltefosine with amiodarone led to a 90% cure in a murine model of leishmaniasis [Serrano-Martin et al., 2009]. The comparison of genome sequences of *Leishmania* spp. and *Trypanosoma* spp. reveals significant differences in their metabolism, mainly related to carbohydrate and amino acid metabolism, and different potential drug targets have been identified in these organisms [Bringaud et al., 2006; Opperdoes and Coombs, 2007].

The pentose phosphate pathway (PPP) plays a central role in metabolism; it is involved in the generation of ribose 5-phosphate and NADPH, which is the major source of reducing power for biosynthetic processes and also maintains the redox potential necessary for protection against oxidative stress [Maugeri and Cazzulo, 2004; Opperdoes et al., 2007]. The 6-Phosphogluconate dehydrogenase (6PGDH; EC 1.1.1.44) is the third enzyme of the oxidative branch of the PPP and has been considered an appropriate target for drugs in trypanosomatids [Barrett and Gilbert, 2002; Hanau et al., 2004; Igoillo-Esteve et al., 2007]. Crystal structures of the 6PGDH enzyme from *Trypanosoma brucei* [Phillips et al., 1998] and *Lactococcus lactis* [Sundaramoorthy et al., 2007] have been elucidated and structural differences have been found in comparison with the mammalian enzymes. A variety of highly selective inhibitors of the enzyme of *T. brucei* has been described [Ruda et al., 2007]. This article focuses on the cloning, expression and biochemical characterization of the 6PGDH from *Leishmania (Leishmania) mexicana* (*Lm*6PGDH). Kinetic studies performed with the recombinant enzyme of *Leishmania* showed kinetic parameter values intermediate between those reported for the enzymes of *T. brucei* and *T. cruzi*. We also deduced the three-dimensional (3D) structures of the 6PGDHs of *Leishmania* and *T. cruzi* (*Tc*6PGDH) by molecular modeling.

Results

Identification of a 6PGDH Gene (Lm6pgdh) *in* L. (L.) mexicana

A putative *Lm6pgdh* gene of *L. (L.) mexicana* was amplified from genomic DNA of *L. (L.) mexicana* using the primer set F2-R1, which generated a PCR product of 1.44 kb, common to strains belonging to the *Leishmania* subgenus; no product was found when genomic DNA from *L. (Viania) braziliensis* or *L. (V.) guyanensis* was used. The PCR product was cloned into the pGEM T Easy vector and subsequently sequenced. The sequence data analysis yielded the open reading frame of the complete *Lm6pgdh* gene (accession No. AY386372), predictive of a polypeptide chain of 479 amino acid residues (accession No. AAQ234), with a molecular mass of 52.0 kDa and a pI of 5.77. Sequence comparison of the *Lm*6PGDH with any of the other 6PGDH available for kinetoplastids revealed a high degree of identity between *Leishmania* spp. (>90%) and *Trypanosoma spp.* (>70%); less than 40% identity was found with the sequence of *Lactococcus lactis* (36%), *Escherichia coli* (37%), *Klebsiella pneumoniae* (36%), *Ovis aries* (34%) and human (36%). Notably, a major difference of 6PGDH between kinetoplastids, bacterial and mammalian proteins, such as sheep and human, was found at the C terminus, where the eukaryotic enzyme has an extension of 12–15 amino acid residues (fig. 1). Southern blot analysis was consistent with the presence of a single gene copy per haploid genome and northern blot analysis showed one band at 2.6 kb (not shown).

Structural Analysis of Lm6*PGDH*

Analysis of the primary structure of the *Lm*6PGDH and comparison with the amino acid sequences from different organisms revealed conservation of the amino acid residues proposed to play important functional roles, including substrate (^{126}ISGG^{129}) and cofactor-binding (^{9}GLGVMG^{14}) sites. An active site, arginine (Arg^{33}), and other key residues located in the catalytic pocket (^{175}GKGGAGSCVKMYHN^{188}) are also conserved (fig. 1). The active form of the enzyme is a dimer, which is stabilized by salt bridge interactions; at least 5 of these salt bridges had been identified in the enzyme of *T. brucei* 6PGDH (*Tb*6PGDH). The *Lm*6PGDH enzyme showed

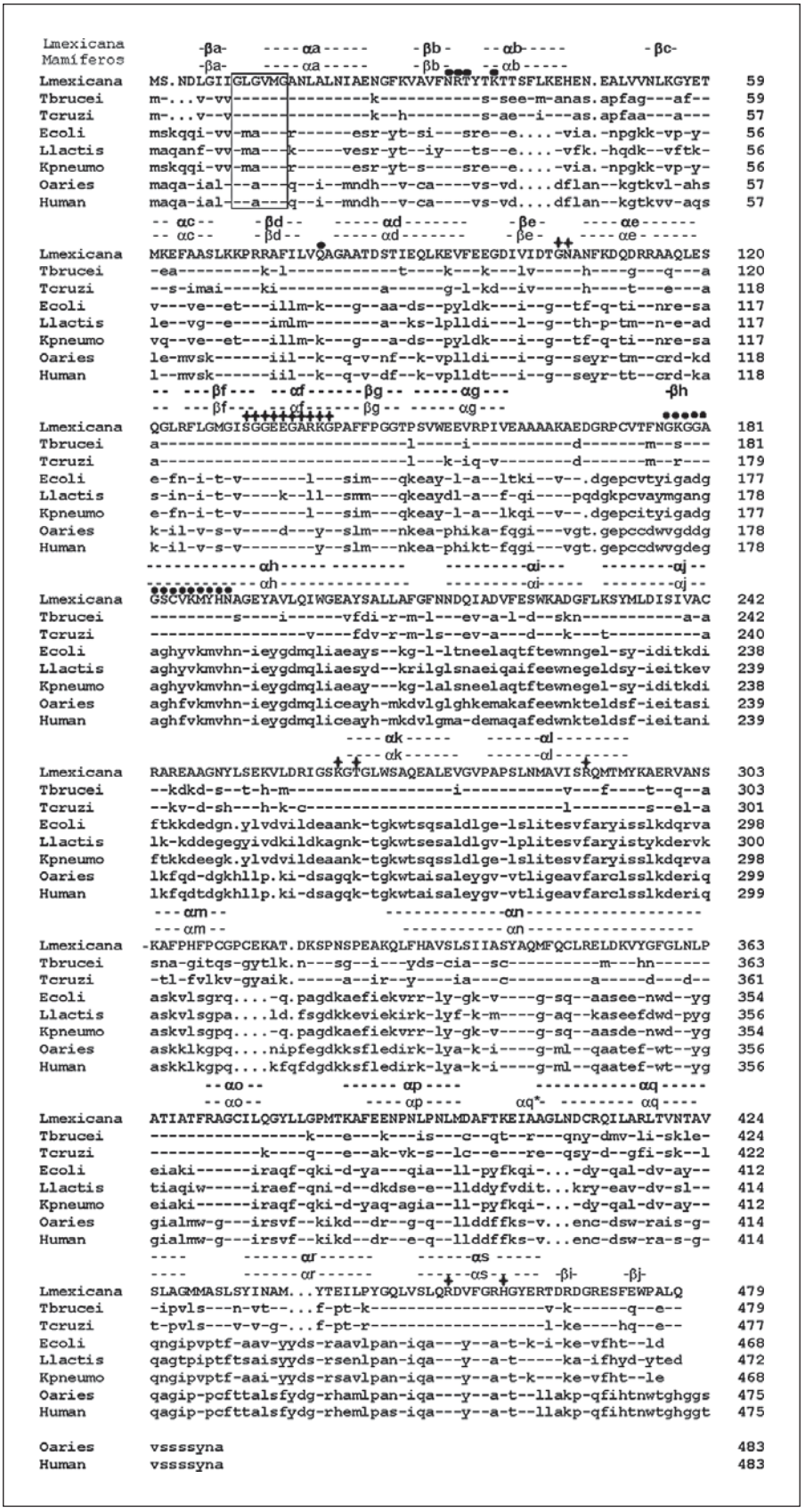

Fig. 1. Multiple alignment of the 6PGDH from different organisms and secondary structure prediction of Lm6PGDH. Predicted amino acid sequences of *L. (L.) mexicana* BEL 21 (AY386372), *T. brucei* (P31072), *T. cruzi* (AY300924), *L. lactis* (AAC12804.1), *E. coli* (AAA23918), *K. pneumoniae* (ABR77917.1), *O. aries* (P00349) and human (P52209) were aligned by the CLUSTAL method. The secondary structure elements are labelled on each block (broken lines) for *O. aries* (first lane) and *L. (L.) mexicana* (second lane); letters on top depict β- and α-strands (βa–βh and αa–αs). Amino acid residues involved in structural domains, previously assigned to β-hydroxyacid dehydrogenases [Njau et al., 2001], are indicated as follows: rectangle (residues 9–14): N-terminal dinucleotide cofactor-binding; oval (residues 32–35, 38 and 76): related residues; asterisks (residues 127–136): substrate-binding; circles (residues 175–188): catalytic site.

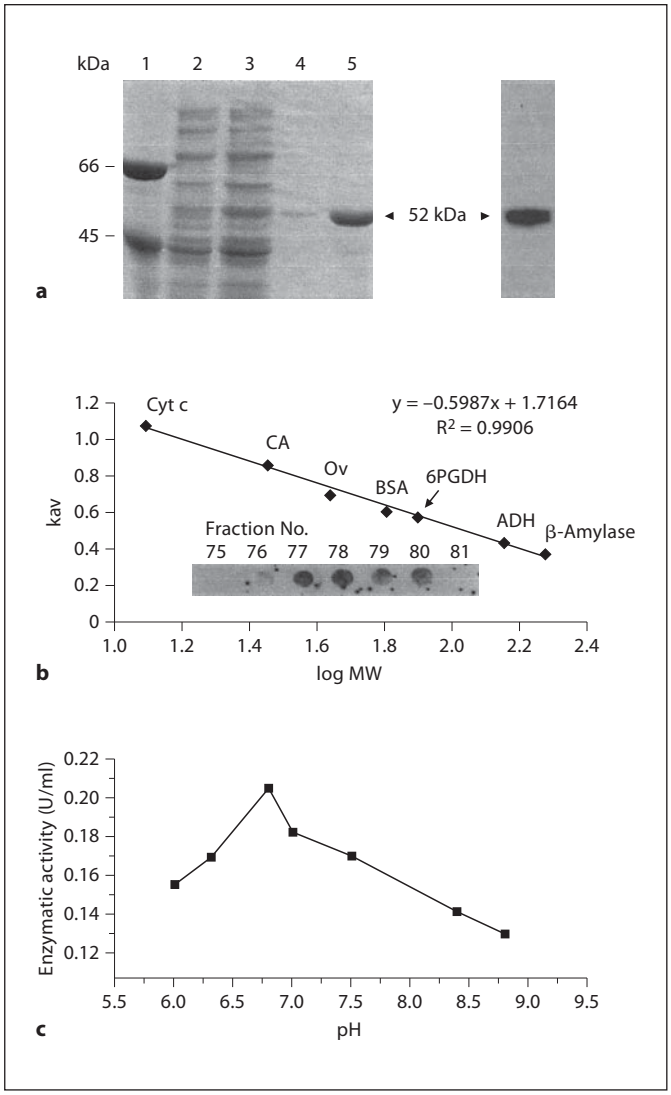

Fig. 2. Purification of recombinant Lm6PGDH. **a** Overexpression and purification of the protein was evaluated by SDS-PAGE and proteins were visualized by Coomassie Blue staining. Lane 1 = molecular markers (bovine serum albumin: 66.0 kDa and ovalbumin: 45.0 kDa); lane 2 = non-induced control cells; lane 3 = induced cells; lanes 4 and 5 = soluble fractions purified by IMAC following elution with 300 mM imidazole. The Lm6PGDH was identified with a polyclonal antiserum raised against the recombinant Tc6PGDH (right). **b** Molecular mass of the active *L. (L.) mexicana* 6PGDH. Molecular mass markers: β-amylase (200 kDa), alcohol dehydrogenase (ADH: 150 kDa), bovine serum albumin (BSA: 66.2 kDa), ovalbumin (Ov: 45 kDa), carbonic anhydrase (CA: 29 kDa) and cytochrome c (Cyt c: 12 kDa). Dot blotting of fractions around 90 kDa (fractions 75–81) was used to develop the Lm6PGDH with the same specific polyclonal antiserum Tc6PGDH (inset). The equation for the regression Kav vs. MW and the determination coefficient are shown. **c** Optimal pH for the active *L. (L.) mexicana* 6PGDH.

substitution of particular amino acid residues related to those involved in salt bridge interaction.

Cloning, Overexpression and Purification of Lm6*PGDH*

The *Lm6pgdh* gene was amplified using the specific primers F2-*Nde I* and R1-*Xho I* and directional cloning was carried out into the expression vector pET28a (+). The recombinant gene was expressed in *E. coli* cells and purified by IMAC. The recombinant *Lm*6PGDH enzyme displayed an apparent molecular mass of 52 kDa on SDS-PAGE and the protein identity was confirmed by immunoblotting using a polyclonal antibody to the *T. cruzi* 6PGDH enzyme (anti-*Tc*6PGDH) (fig. 2a). A molecular mass of 90 kDa was found for the recombinant protein following separation on a Sephacryl S300 gel filtration column (fig. 2b). The *Lm*6PGDH enzyme was identified by immuno-dot blot using anti-*Tc6*PGDH antibodies (fig. 2b, inset). This result established that the *Lm*6PGDH enzyme is a dimer in its native state.

After 30 min elution from the IMAC column, we observed a severe decrease (>90%) in enzymatic activity of the recombinant enzyme *Lm*6PGDH at high concentration of imidazole (300–100 mM). In order to preserve enzyme activity, at least for 24 h, it was necessary to reduce imidazole concentration to 50 mM, and adjust the solution to a final concentration of 5 mM β-mercaptoethanol; however, these conditions were not appropriate for establishing the kinetic parameters. Since freezing and thawing of the enzyme solution reduced enzyme activity in 90%, the solution was stored at 4°C.

Biochemical Properties: Kinetic Studies

Maximum enzymatic activity was found at pH 6.8 after incubation for 10 min of the purified recombinant enzyme in buffer 50 mM Tris-HCl, 250 mM NaCl, 50 mM imidazole and 5 mM β-mercaptoethanol (fig 2c). A marked inactivation at alkaline pH was found for the *Lm*6PGDH, more than 60% activity being lost.

The inactivation of a substantial amount of the protein during the purification process affected the determination of the biochemical properties of the enzyme. In order to minimize the effect of imidazole on the loss of enzyme activity, we evaluated different buffers without this reagent; 50 mM Tris-acetate buffer pH 7.0 was chosen for the kinetic studies. The recombinant *Lm*6PGDH displayed standard Michaelis-Menten kinetics and the corresponding Lineweaver-Burke plots showed K_m values for 6PG and $NADP^+$ of 6.93 μM and 5.20 μM, respectively (table 1). The *Lm*6PGDH displayed kinetic parameter

values intermediate to those described for the recombinant *Tb*6PGDH and *Tc*6PGDH. The low values of the kinetic parameters of *Lm*6PGDH were in contrast with those of the human enzyme (table 1), suggesting sufficient differences between these enzymes.

Molecular Modelling

The sequence of *Lm*6PGDH was aligned with the homologous 6PGDH of *T. brucei* (PDB: 1PGJ), *L. lactis* (PDB: 2IYP), sheep (PDB: 2PGD) and human (PDB: 2JKV). The structural model of *Lm*6PGDH was established using *Tb*6PGDH (PDB: 1PGJ chains A an B) as template, based on sequence identity (72%). The *Lm*6PGDH protein is a homodimer and the structure of the model of monomers, 6pgdhA and 6pgdhB, was generated by the SWISS-MODEL package (fig. 3a). Three main domains were identified in the monomer structure of *Leishmania*: I, the coenzyme domain, residues 1–178; II, the helix domain, residues 179–441, and III, the tail, residues 442–478; similar results were found for *Tc*6PGDH. Comparison of the homology model of *Lm*6PGDH with that of *Tb*6PGDH and *Tc*6PGDH and also with *Tc*6PGDH and *Tb*6PGDH (not shown) suggested a similar structure for the 6PGDH monomer in these kinetoplastids. Nevertheless, differences were found between them and with the crystal structure of the human 6PGDH enzyme (fig. 3b).

The quality of the *Lm*6PGDH and *Tc*6PGDH model was established by superimposition on the crystal structure of the template and the estimated value of root mean-square deviation (RMSD) was 0.08 Å for the Cα atoms, suggesting minimal or no deviation of our model from the template; also, examination of the Ramachandran plot (not shown) indicated a good overall geometry for the *Leishmania* model (table 2). The energy of protein folding of the monomers in the structural model of *Lm*6PGDH showed typical features of a native structure with a z-score value of –10.13 (A monomer) and –10.08 (B monomer). A value of potential energy of –49,948.1 kJ/mol was obtained for the dimeric model, which was similar to the value for the *T. brucei* protein (–50,385.9 kJ/mol). In general, the structural features of the *Tc*6PGDH model were similar to those described for the model of *Leishmania* (table 2).

Since the active form of the enzyme has been described as a dimer, a model of its structure was also generated. The homology model of *Lm*6PGDH was compared with the crystal structure of the human 6PGDH recently reported (PDB: 2JKV); superimposition of both structures showed higher similarities (fig. 3c) with an RMSD of 4.09 Å (table 2). Nevertheless, significant differences were identified between human and *Lm*6PGDH. A comparison of both the active site and the cofactor-binding site of the 6PGDH was performed (fig. 3d); in the active site, no major differences were observed. The site is a cleft surrounded by residues from all 3 domains. In the coenzyme-binding domain of *Lm*6PGDH, in contrast to the human enzyme, a significant change involving 7 amino acid residues was observed: ^{31}Phe, ^{32}Asn, ^{33}Arg, ^{34}Thr, ^{35}Tyr, ^{36}Thr and ^{37}Lys. The C- terminal tail in the human 6PGDH is longer than in the structural model of *Lm*6PDGH and the coenzyme-binding domain is occluded.

Table 1. Kinetic parameters of the recombinant *Lm*6PGDH

Species	K_m (μM)	
	6PG	$NADP^{+a}$
L. (L.) mexicana	6.93	5.2
T. brucei	3.5	1.5
T. cruzi	22.2	5.9
Human	20.0	30.0

[a] Igoillo-Esteve and Cazzulo, 2004.

Dimerization of the 6PGDH involves particular amino acid residues of the C-terminal region of the monomers in the establishment of salt bridges. For instance, 5 of these bridges are present in the dimeric form of *Tb*6PGDH enzyme (fig. 4); however, by comparison, we found 4 potential salt bridges in *Leishmania*: ^{459}Arg-^{134}Glu (bridge 1) in the coenzyme domain and ^{463}Glu-^{259}Arg (bridge 3), ^{464}Arg-^{246}Glu (bridge 4) and ^{466}Asp-^{255}Lys (bridge 5), in the helical domain (fig. 4). Analysis of the pocket structure of the active site of the *Lm*6PGDH enzyme and evaluation of the distance between other amino acid residues involved in salt bridges suggest the absence of bridge 5 in *Leishmania* due to the large distance, 6.73 v. 4.53 Å, between the residues involved. In *T. cruzi,* salt bridges 3 and 4 in the helical domain are absent (fig. 4).

Discussion

We have successfully identified, cloned, expressed and established a structural homology model of the *Lm*6PGDH. Southern blot analysis suggested a single

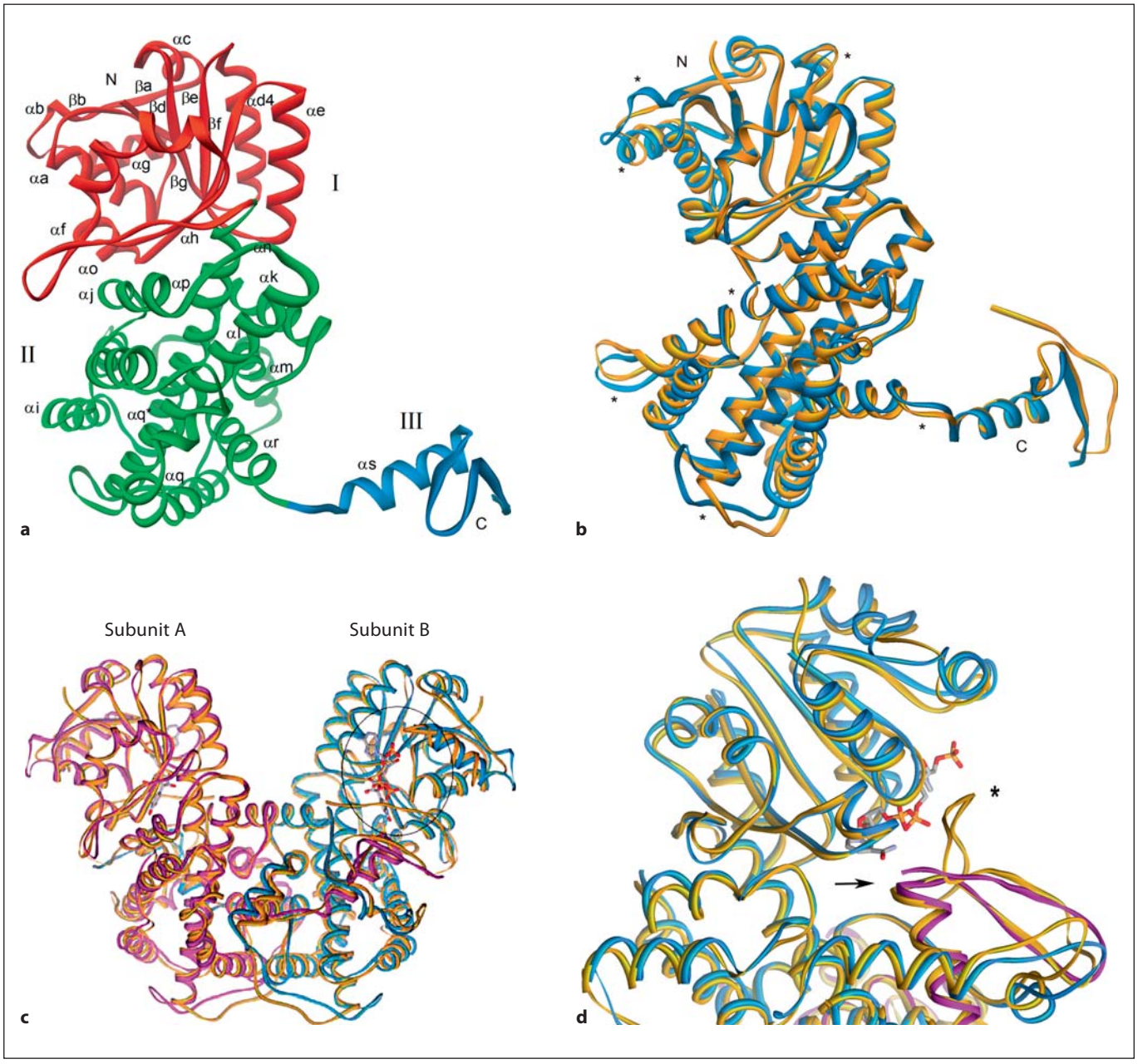

Fig. 3. Comparison of the homology model of *Lm*6PGDH and human 6PGDH. **a** Ribbon diagram of an *Lm*6PGDH monomer. Three domains are described: I: the cofactor binding domain or N-terminal coenzyme (residues 1–178, red); II: helix domain (residues 179–441, green), and III: tail domain (residues 442–478, blue). Secondary structure elements (helices α, αf, j, k, etc. and strands βa, b, etc.) are labeled according to the domain. The N and C termini are marked. **b** Monomers of *L. (L.) mexicana* (blue) and human 6PGDH (gold) are superimposed; regions showing significant differences are marked (*). **c** Superimposition of 6PGDH dimers of *L. (L.) mexicana* (subunit A, magenta; subunit B, blue) and human (gold). Circle shows the NADPH in the coenzyme-binding domain. **d** Interactions of the NADPH are shown as ball-and-stick, in the coenzyme-binding domain of *L. (L.) mexicana* and human (gold) 6PGDH enzyme. The arrow points at the cofactor-binding pocket.

Table 2. Structure comparison of the Lm6PGDH model with different organisms

	L. (L.) mexicana	*T. brucei*	*T. cruzi*	*L. lactis*	*O. aries*	*Human*
PDB code	–	1PGJ	–	2IYP	2PGD	2JKV
Number of residues	474	478	476	469	473	505
Sequence identity with *L. (L.) mexicana*	–	72%	72%	37%	34%	36%
RMSD Cα versus *L. (L.) mexicana*	–	0.08 Å (474 Cα atoms)	0.05 Å (474 Cα atoms)	1.33 Å (469 Cα atoms)	1.30 Å (473 Cα atoms)	4.09 Å (462 Cα atoms)
Total area, Å^2 Total volume, Å^3	28,840 128,054	28,629 128,773	29,282 128,342	28,603 12,883	28,894 128,163	29,330 129,164
%phi/psi[a]	92	91	92	93	96	93
Energy, kJ/mol	–49,948.1	–50,385.9	–48,943.7	–52,811.9	–34,868.6	–49,539.8
Energy, kJ/mol[b] (in silico mutant)	–52,902.5	–	–53,330.9	–	–	–

PDB = Protein data bank code; RMSD = root-mean-square deviation; Cα = α-carbon.
[a] Phi and psi are torsion angle of the all residues of the 6PGDH chain, %phi/psi: phi-psi combination in favourable regions of the Ramachandran plot.
[b] Energy value of model where restoration of salt bridges was carried out by in silico mutation.

copy of the *Lm6pgdh* gene, which coded for a polypeptide chain of 479 amino acid residues, in agreement with that established through the genome project of *Leishmania* and also described for *L. (L.) major* [Greenblatt et al., 2002], *T. brucei* [Barrett and Le Page, 1993] and *T. cruzi* [Igoillo-Esteve and Cazzulo, 2004]. A high sequence identity of 6PGDH was found among trypanosomatids. The secondary structure assignment of the *Lm*6PGDH protein showed high similarity with that of *T. brucei*, differences arising from the absence or modification in the *Leishmania* enzyme of particular residues involved in the secondary structures such as *Tb*βc and *Tb*αj* (small 3_{10} helix present in *T. brucei* but absent in sheep 6PGDH) [Phillips et al., 1998].

The folding pattern similarities found between the monomer models of *Lm*6PGDH and of *Tc*6PGDH with the 3D structure of the *Tb*6PGDH established by X-ray were striking [Hanau et al., 2004; Phillips et al., 1998]. Comparison of the RMSD values suggests a high degree of structural conservation of the 6PGDH enzyme between *Leishmania*, *T. brucei* and *T. cruzi* and significant differences in structure to its mammalian counterpart [Phillips et al., 1998].

The active form of the enzyme has been described as a dimer and comparison of the amino acid residues among *Leishmania, T. cruzi* and the 3D structure of the *Tb*6PGDH, showed the conservation of a common salt bridge established between charged amino acid residues ^{459}Arg and ^{134}Glu (bridge 1). It has been predicted that bridge 1 is a feature of those 6PGDH enzymes that do not have the glycine-serine-rich C-terminal extension, as in the case of the enzymes of trypanosomatids [Phillips et al., 1998]. Other salt bridge interactions, present in *T. brucei* enzyme, are conserved in *Leishmania*, such as amino acid residues involved in bridge 3 and bridge 4, although in the latter ^{246}Asp is replaced by ^{246}Glu in *Leishmania*. There are other changes in *Leishmania*, which lead to the loss of the interaction of amino acid residues involved in the formation of two other salt bridges described in the coenzyme domain of the *T. brucei* enzyme; these changes include substitution of a negatively charged residue (^{477}Glu) for a nonpolar one (^{477}Ala) (bridge 2), and a positively charged residue (^{255}His) for a similar one (^{255}Lys, bridge 5).

Specific alterations occurred in residues that interact directly with the coenzyme and also in the helical domain, e.g. those residues that diminish the number of salt bridges and may affect the affinity for the coenzyme and the stability of the enzyme. Instability of native and recombinant 6PGDH enzyme of *T. cruzi* has been associated with the absence of two of the bridges (bridges 3 and 4) described in the helical domain of *T. brucei*; the stability of the enzyme was recovered by the use of site-directed mutagenesis to restore the salt bridges [Igoillo-Esteve and Cazzulo, 2004]. In fact, restoration of salt bridges 3 and 4 in the model of *T. cruzi* 6PDGH by in silico site-

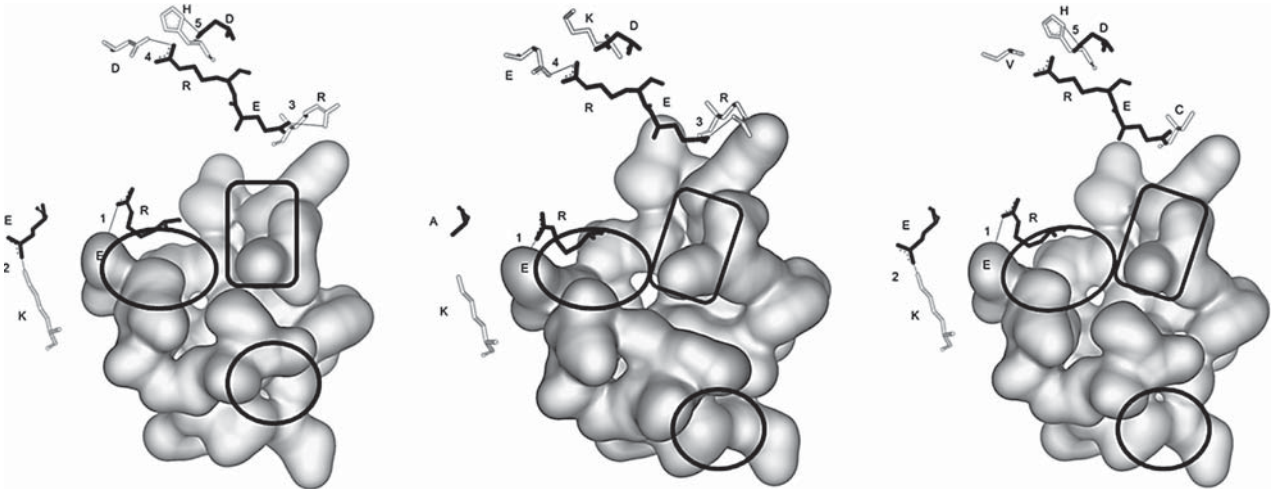

a

	T. brucei	*L. (L.) mexicana*	*T. cruzi*
Coenzyme Domain	**(1)** Arg^{459}-Glu^{134} 4.73/4.08	Arg^{459}-Glu^{134} 4.86/3.87	Arg^{459}-Glu^{134} 4.73/3.97
	(2) Glu^{477}-Lys^{139} 4.46/4.99	**NB**	Glu^{477}-Lys^{139} 4.50/5.01
Helical Domain	**(3)** Glu^{463}-Arg^{259} 3.74/2.95	Glu^{463}-Arg^{259} 4.09/3.06	**NB**
	(4) Arg^{464}-Asp^{246} 2.76/3.06	Arg^{464}-**Glu**^{246} 4.70/3.23	**NB**
	(5) Asp^{466}-His^{255} 3.70/3.22	Asp^{466}-**Lys**^{255} **6.73/4.53**	Asp^{466}-His^{255} 3.67/3.23

b

Fig. 4. Amino acid residues involved in salt bridge interactions between 6PGDH monomers. **a** The active-site pocket of 6PGDH enzyme of *T. brucei*, *Leishmania* and *T. cruzi* was modelled according to the electrostatic potential of the surface [using the CASTp service (http://sts.bioengr.uic.edu/castp/about.php)]. **b** The amino acid residues involved in salt bridges were numbered according to the bridges established for *T. brucei* (1–5) used as a reference. Numbers under amino acid residues correspond to the distance (Å) between monomers, subunit A–B and B–A, respectively. Electronic density charge: negative (oval), positive (rectangle). Hydrophobic surface (grey). NB = No bridge.

direct mutagenesis generated a new model with all 5 salt bridges present in the wild-type enzyme of *T. brucei*, which showed a value of potential energy (–53,330.90 kJ/mol) lower than that obtained when the bridges were absent (–48,943.70 kJ/mol; see table 2), in agreement with the recovery of enzyme stability by biological mutagenesis experiments. We also found instability of the native and recombinant enzymes in *Leishmania,* albeit to a lesser extent than in the case of *T. cruzi*. We speculated that, as in *T. cruzi,* the absence of 2 salt bridges probably relates to this instability of the *Lm*6PGDH. As in *T. cruzi*, restoration of the salt bridges on the *Lm*6PGDH model by in silico mutagenesis reduced the potential energy of the dimeric model from –49,948.1 to –52,902.5 kJ/mol (table 2), suggesting higher enzyme stability.

In summary, the results include the first homology model for the *Lm*6PGDH whose structural features, such as the RMSD, suggest a minimal or no deviation from the crystal structure of the enzyme of *T. brucei*. Significant differences with *T. brucei* and *T. cruzi* were found in amino acid residues of *Leishmania* involved in the inter-subunit salt bridges for dimerization, probably related to the low stability of the enzyme. Differences in structure of the 6PGDH enzyme of trypanosomatids when compared

with its mammalian counterpart, such as the human enzyme, are currently exploited for the evaluation of small-molecule inhibitors through virtual screening by molecular docking.

Experimental Procedures

Leishmania *Culture*

The *Leishmania* strains used in this study, identified as *L. (L.) mexicana*, were the strains M379 (YC/BZ/62/M379) and BEL21 (MHOM/BZ/82/BEL21), considered as reference strains by WHO, and the Venezuelan strain M9012 [Luis et al., 1998]. For all analyses, promastigotes were grown at room temperature in Schneider's *Drosophila* medium (Gibco) supplemented with 10% heat-inactivated fetal calf serum and 100 μg/ml kanamycin [Mendoza-León et al., 2002]. The parasite pellet (3×10^9 total parasites) was resuspend in 2 ml cold TMD buffer (50 mM Tris pH 7.6, 10 mM $MgCl_2$, 1 mM dithiotreitol) in the presence of a cocktail of protease inhibitors (1% v/v protease cocktail-Sigma P2414).

DNA Extraction, Amplification, Sequencing and Analysis of Lm6pgdh

Genomic DNA was extracted from promastigotes as previously described [Luis et al., 1998]. The putative *Lm6pgdh* gene was amplified from the genomic DNA of *L. (L.) mexicana* using oligonucleotides designed after the in silico identification of overlapping nucleotide sequences encoding the *6pgdh* gene from *L. (L.) major* (accession No. AAF64172, AF242437 and AF242436), *L. (L.) tropica* (accession No. AY045763) [Greenblatt et al., 2002], *T. cruzi* (accession No. AY300924) and *T. brucei* (accession No. P31072); these sequences were screened with *Leishmania* genome project data bases. The primer F2 (5′-ATgTCgAACgACCTCggCATT-3′; T_m: 64.3°C) and R1 (5′-TTACTgCAgTgCgggCCATTCg-3′; Tm: 67.8°C) were used as forward and as reverse, respectively. The PCR was performed in a final volume of 25 μl, containing the cocktail of PCR-Master mix (Promega), primers at 0.4 μM and 10 ng DNA, in an MJ Research PTC200 thermocycler. The PCR settings were 5 min of pre-incubation at 95°C and 40 cycles under the following conditions: 95°C for 1 min, 55°C for 1 min and 72°C for 2 min; a final extension step at 72°C for 10 min was included. A single PCR product of 1.4 kb was generated upon agarose gel purification and the product was directly sequenced on an Analysis Sequencer (Perkin-Elmer ABI PRISM 377). Sequence analysis was performed using the BLAST method, and multiple alignments were done with the CLUSTAL method [Thompson et al., 1994]. Protein sequences were retrieved from the SwissProt database.

Cloning of Lm6pgdh

The restriction sites *Nde* I and *Xho* I (underlined) were included in primers F2 and R1 to facilitate the directional cloning of the *Lm6pgdh* gene into the expression vector, F2-*Nde* I (5′-GGGAATTCCAT**ATG**TCGAACGACCTCGGCATT-3′; Tm: 64.3°C) and R1-*XhoI* (5′-CCGCTCGAGTTACTGCAGTGCGGGCCATTCG-3′; Tm: 67.8°C). The 1.4-kb PCR product generated *(Lm6pgdh)* was cloned into the pGEM-T Easy vector (Promega) for sequencing. Thereafter, the *Lm6pgdh* gene was removed by digestion with both *Nde* I and *Xho* I restriction enzymes and cloned into the *Nde* I-*Xho* I site of pET28a(+) expression vector (Novagen, Darmstadt, Germany). The new construct was fully sequenced and used to transform *E. coli* BL21-codon plus (DE3) strain; a single bacterial colony was grown overnight at 37°C in LB medium supplemented with 50 μg/ml kanamicin and 10 μg/ml chloramphenicol.

Overexpression and Purification of Recombinant 6PGDH

For recombinant protein expression, a single bacterial colony was grown overnight at 37°C in LB medium supplemented with 50 μg/ml kanamicin and 10 μg/ml chloramphenicol; the culture was diluted 1:50 with the same medium and grown at 37°C. When the culture reached an optical density of 0.6 at 600 nm, protein induction with isopropyl-β-D-thiogalactopyranoside was performed according to procedures described previously [Igoillo-Esteve and Cazzulo, 2004].

Molecular Mass

The molecular mass of the active *L. (L.) mexicana* 6PGDH recombinant $(His)_6$-tagged protein was determined by gel filtration in a Sephacryl S300 column [total volume (V_t): 53 ml] equilibrated with 50 mM Tris-HCl pH 7.0, 250 mM NaCl, 10 mMMg_2Cl and 1 mM DTT, employing a flow rate of 150 μl/min. The column was calibrated with standard molecular markers and the molecular mass determined as previously reported [Camargo et al., 2004]. Fractions containing *Lm*6PGDH were identified by dot blot on nitrocellulose membrane (Hybond ECL, Amersham Biosciences) using a rabbit anti-Tc-6PGDH; previously, the nitrocellulose membrane was blocked with 1 × PBS, 5% (w/v) skimmed milk for 2 h; the membrane was incubated with polyclonal antibodies for Tc-6PGDH. The membrane was washed and incubated for 1 h with a secondary antibody, the anti-rabbit horseradish peroxidase conjugate 1:10,000 (Sigma). Immunoblot was developed as previously described [Igoillo-Esteve and Cazzulo, 2006].

Enzyme Assays and Kinetic Parameters

Routinely, the enzymatic activity of 6PGDH was measured spectrophotometrically at room temperature in a Beckman DU Series 750 spectrophotometer, monitoring the reduction of $NADP^+$ at 340 nm and room temperature [Cronin et al., 1989]. The standard assay mixture contained 50 mM triethanolamine buffer pH 7.5, 5 mM $MgCl_2$, 1 mM 6PG and 0.5 mM $NADP^+$, to a final volume of 100 μl.

The optimal pH for the activity of the recombinant enzyme was determined under previously described conditions [Igoillo-Esteve and Cazzulo, 2004]. The kinetic parameters of the recombinant *L. (L.) mexicana* 6PGDH enzyme were determined by varying the concentration of each substrate over a range of 3–25 μM for $NADP^+$, and of 10–100 μM for 6PG, keeping the other substrate at saturating concentrations (1 mM for 6PG and 0.5 mM for $NADP^+$). The mixture contained 50 mM Tris acetate buffer, pH 7.0, 10 mM $MgCl_2$ and the reaction was initiated by the addition of the enzyme at room temperature to a final volume of 0.1 ml. Protein concentration was estimated by the Bradford method, using serum albumin as standard.

Molecular Modelling

A homology model of the *Leishmania* 6PGDH, and also of the *T. cruzi* enzyme, was generated using as template the chain A

(PDB 1PGJA) and B (PDB 1PGJB) of the crystal structure of the 6PGDH from *T. brucei* and the SWISS-MODEL modelling server (http://swissmodel.expasy.org/SWISS-MODEL.html) [Schwede et al., 2003]. The dimer was generated using the tools of the DeepView/Swiss-PdbViewer 4.01 program (GlaxoSmithKline). A second model including all 5 salt bridges that are present in the wild type of *T. brucei* 6PGDH was generated to *Leishmania* and *T. cruzi* 6PGDH by in silico site-direct mutagenesis, followed by minimization procedures. Specific point mutations involve ^{477}Ala→^{477}Glu, ^{246}Glu→^{246}Asp and ^{255}Lys→^{255}His for *Leishmania*; and, ^{259}Cys→^{259}Arg and ^{246}Val→^{246}Asp for *T. cruzi*.

The model refining was carried out using the DeepView/Swiss-PdbViewer 4.01 program (GlaxoSmithKline), and subjected to energy minimization using the Gromos 43B1 force field (Groningen Molecular Simulation System). The figures of the models were viewed by the WebLab ViewerLite 3.20 (MSI/Accelrys) and DeepView/Swiss-PdbViewer 4.01 programs [Guex and Peitsch, 1997]. The validation of the generated homology models was carried out with ProSA [Wiedertein and Sippl, 2007], and What If programs [Vriend, 1990] (https://prosa.services.cama.sbg.ac.at/prosa.php & http://swift.cmbi.ru.nl/servers/html/index.html). The energy of the folding, geometry and stoichiometry of the models were evaluated by means of the ProSA-web and What If services (https://prosa.services.cama.sbg.ac.at/prosa.php & http://swift.cmbi.ru.nl/servers/html/index.html).

Nucleotide and amino acid sequence data reported in this paper are available in the GeneBank databases under the accession numbers: *L. (L.) mexicana* **AY386372**; *T. brucei* P31072; *T. cruzi* AY300924; *E. coli* AAA23918; *K. pneumoniae* ABR77917.1; *L. lacticus* AAC12804.1; *O. aries* P00349; and human P52209.

Acknowledgements

The authors are grateful to Dr. Ana Herrera (IBE-UCV) for her critical comments. This work was funded by the European Commission INCO-DC programme and CDCH-UCV, and partial funds from grants Fonacit 2000001639 and Misión Ciencia 2007000960–2 to J.B. D.G. had Venezuelan fellowships from the CDCH-UCV and FONACIT, and received financial support from UNU-BIOLAC to visit J.J. Cazzulo's laboratory.

References

Barrett MP, Gilbert IH: Perspectives for new drugs against trypanosomiasis and leishmaniasis. Curr Top Med Chem 2002;2:471–482.

Barrett MP, Le Page RWF: A 6-phospho-gluconate dehydrogenase gene from *Trypanosoma brucei*. Mol Biochem Parasitol 1993;57:89–100.

Bringaud F, Riviere L, Coustou V: Energy metabolism of trypanosomatids: adaptation to available carbon sources. Mol Biochem Parasitol 2006;149:1–9.

Camargo RE, Uzcanga GL, Bubis J: Isolation of two antigens from *Trypanosoma evansi* that are partially responsible for its cross-reactivity with *Trypanosoma vivax*. Vet Parasitol 2004;123:67–81.

Coler RN, Reed SG: Second-generation vaccines against leishmaniasis. Trends Parasitol 2005;21:244–249.

Croft SL, Barrett MP, Urbina JU: Chemotherapy of trypanosomiases and leishmaniasis. Trends Parasitol 2005;21:508–512.

Croft SL, Coombs GH: Leishmaniasis-current chemotherapy and recent advances in the search for novel drug. Trends Parasitol 2003;19:502–508.

Cronin CN, Nolan DP, Voorheis HP: The enzymes of the classical pentose phosphate pathway display differential activities in procyclic and bloodstream forms of *Trypanosoma brucei*. FEBS Lett 1989;244:26–30.

Davis AJ, Murray HW, Handman E: Drug against leishmaniasis: a synergy of technology and partnerships. Trends Parasitol 2004;20:73–76.

Greenblatt ChL, Schnur LF, Bar-Gal GK, Ermolaev H, Peleg N, Barrett MP: Polymorphism among alleles of the 6-phosphogluconate dehydrogenase gene from *Leishmania major* and *Leishmania tropica*. Mol Biochem Parasitol 2002;125:185–188.

Guex N, Peitsch MC: SWISS-MODEL and the Swiss-PdbViewer: an environment for comparative protein modeling. *Electrophoresis* 1997;18:2714–2723.

Hanau S, Rinaldi E, Dallocchio F, Gilbert IH, Dardonville Ch, Adams MJ, Gover S, Barrettt MP: 6-Phosphogluconate dehydrogenase: a target for drug in African trypanosomes. Curr Med Chem 2004;11:2639–2650.

Igoillo-Esteve M, Cazzulo JJ: The 6-phosphogluconate dehydrogenase from *Trypanosoma cruzi*: the absence of two inter-subunit salt bridges as a reason for enzyme instability Mol Biochem Parasitol 2004;133:197–207.

Igoillo-Esteve M, Cazzulo JJ: The glucose-6-phosphate dehydrogenase from *Trypanosoma cruzi*: its role in the defense of the parasite against oxidative stress. Mol Biochem Parasitol 2006;149:170–181.

Igoillo-Esteve M, Maugeri D, Stern AL, Beluardi P, Cazzulo JJ: The pentose phosphate pathway in *Trypanosoma cruzi*: a potential target for the chemotherapy of Chagas disease. An Acad Bras Cienc 2007;79:649–663.

Luis L, Ramirez A, Aguilar CM, Eresh S, Barker DC, Mendoza-León A: The genomic fingerprinting of the coding region of the β-tubulin gene in *Leishmania* identification. Acta Trop 1998;69:193–204.

Maugeri DA, Cazzulo JJ: The pentose phosphate pathway in *Trypanosoma cruzi*. FEMS Microbiol Lett 2004;234:117–123.

Mendoza-León A, Luis L, Martinez C: The β-tubulin gene region as a molecular marker to distinguish *Leishmania* parasites; in Aquino de Muro M, Rapley R (eds). Methods in Molecular Biology. Gene Probes – Principles and Protocols. Totowa, NJ, Humana Press Inc., 2002, vol 179, pp 61–83.

Njau RK, Herndon CA, Hawes JW: New developments in our understanding of the β-hydroxyacid dehydrogenase. Chem Biol Interactions 2001;130–132:785–791.

Opperdoes FR, Coombs GH: Metabolism of *Leishmania*: proven and predicted. Trends Parasitol 2007;23:149–158.

Ouellette M, Drummelsmith J, Papadopoulou B: Leishmaniasis: drug in the clinic, resistance and new developments. Drug Resist Updates 2004;7:257–266.

Phillips C, Dohnalek J, Gover S, Barrett MP, Adams MJ: A 2.8-Å resolution structure of 6-phosphogluconate dehydrogenase from the protozoan parasite *Trypanosoma brucei*: comparison with the sheep enzyme accounts for differences in activity with coenzyme and substrate analogues. J Mol Biol 1998;282:667–681.

Ruda GF, Alibu VP, Mitsos Ch, Bidet O, Kaiser M, Brun R, Barrett MP, Gilbert IH: Synthesis and biological evaluation of phosphate prodrugs of 4-phospho-D-erythronohydroxamic acid, an inhibitor of 6-phosphogluconate dehydrogenase. Chem Med Chem 2007;2: 1169–1180.

Schwede T, Kopp J, Guex N, Peitsch MC: SWISS-MODEL: an automated protein homology-modeling server. Nucleic Acids Res 2003;31: 3381–3385.

Serrano-Martín X, Payares G, De Lucca M, Martínez JC, Mendoza-León A, Benaim G: Amiodarone and miltefosine act synergistically against *Leishmania mexicana* and can induce parasitological cure in a murine model of cutaneous leishmaniasis. Antimicrob Agents Chemother 2009;53:5108–5113.

Sundaramoorthy R, Iulek J, Barrett MP, Bidet O, Ruda GF, Gilbert IH, Hunter WN: Cristal structure of a bacterial 6-phosphogluconate dehydrogenase reveal aspects of specificity, mechanism and mode of inhibition by analogoues of high-energy reaction intermediates. FEBS J 2007;274:275–286.

Thompson JD, Higgins DG, Gibson TJ: CLUSTAL W Improving the sensitivity of progressive multiple sequence alignment through sequence weighting, position-specific gap penalties and weight matrix choice. Nucleic Acids Res 1994;22:4673–4680.

Vriend G: WHAT IF: A molecular modeling and drug design program. J Mol Graph 1990;8: 52–56.

Wiederstein M, Sippl MJ: ProSA-web: interactive web service for the recognition of errors in three-dimensional structures of proteins. Nucleic Acids Res 2007;35:W407–W410.